J Porous Mater (2008) 15:601–611
DOI 10.1007/s10934-007-9139-x

The influence of carbon source on the wall structure of ordered mesoporous carbons

Yunpu Zhai · Ying Wan · Yan Cheng · Yifeng Shi · Fuqiang Zhang · Bo Tu · Dongyuan Zhao

Received: 12 March 2007 / Accepted: 21 May 2007 / Published online: 20 July 2007

Abstract A series of ordered mesoporous carbons (OMCs) have been synthesized by filling the pores of siliceous SBA-15 hard template with various carbon precursors including sucrose, furfuryl alcohol, naphthalene and anthracene, followed by carbonization and silica dissolution. The carbon replicas have been characterized by powder XRD, TEM and N_2 adsorption techniques. Their electrochemical performance used as electric double-layer capacitors (EDLCs) were also conducted with cyclic voltammetry and charge-discharge cycling tests. The results show that highly ordered 2D hexagonal mesostructures were replicated by using all these four carbon sources under the optimal operation conditions. Physical properties such as mesoscopic ordering, surface areas, pore volumes, graphitic degrees, and functional groups are related to the precursors, but pore sizes are shown minor relationship with them. The sources, which display high yields to carbons, for example, furfuryl alcohol and anthracene are favorable to construct highly ordered mesostructures even at high temperatures (1300 °C). OMCs prepared from non-graphitizable sources such as sucrose and furfuryl alcohol display amorphous pore walls, and large surface areas and pore volumes. The functional groups in the precursors like sucrose and furfuryl alcohol can be preserved on carbon surfaces after the carbonization at low temperatures but would be removed at high temperatures. The graphitizable precursors with nearly parallel blocks and weak cross-linkage between them like anthracene are suitable for deriving the OMCs with graphitic walls. Therefore, the OMCs originated from sucrose and furfuryl alcohol behave the highest capacitances at a carbonization of 700 °C among the four carbons due to the high surface areas and plenty of functional groups, and a declination at high temperatures possibly attribute to the depletion of functional groups. Anthracene derived OMCs has the lowest capacitance carbonized at 700 °C, and a steady enhancement when heated at high temperatures, which is attributed to the graphitization. The OMCs derived from naphthalene have the stable properties such as relatively high surface areas, few electroactive groups and limited graphitizable properties, and in turn medium but almost constant capacitances.

Keywords Mesoporous carbon · Nanocasting · Mesoporous silica · SBA-15

Y. Zhai · Y. Wan · Y. Cheng · Y. Shi · F. Zhang · B. Tu · D. Zhao (✉)
Department of Chemistry, Shanghai Key Laboratory of Molecular Catalysis and Innovative Materials, Key Laboratory of Molecular Engineering of Polymers of the Chinese Ministry of Education, Laboratory of Advanced Materials, Fudan University, Shanghai 200433, P.R. China
e-mail: dyzhao@fudan.edu.cn

Y. Wan
Department of Chemistry, Shanghai Normal University, Shanghai 200234, P.R. China

1 Introduction

Ordered mesoporous carbons (OMCs) have attracted lots of interest since the first report of CMK-1 casted from mesoporous silica MCM-48 in 1999 [1], because of both the remarkable properties such as high surface areas, monodisperse pores of well defined size and mesostructures, and the operable synthesis like diverse carbon sources, good reproducibility and high yields. This method later on stimulated many enthusiasms on research. A series of OMCs with different mesostructures, e.g. CMK-2 [2], CMK-3 [3], CMK-4 [4] with cubic $Pm\bar{3}n$, $Ia\bar{3}d$ and

hexagonal *p*6 *mm* symmetries, respectively, have been fabricated from mother mesoporous silica with corresponding structures. These carbon materials show wide applications in the fields of electrochemistry, hydrogen storage, catalysis, sensors and adsorption, etc [5–8].

The understanding and control of both the mesostructure and the microstructure including symmetry, pore size and graphitization are no less critical for significant progress in their practical applications. Indeed, it could be argued that OMCs casted by mesoporous silicas from laboratories and even from batches are dissimilar in physical and chemical characters, for example, BET surface areas and pore sizes. Many results differ much with each other. It is mainly because of the multi-step synthesis. This nanocasting procedure for ordered mesoporous carbons can be outlined as: (1) preparation of the mesoporous silica as the hard template, (2) introduction of the carbon source into channels of mesoporous silica through impregnation or chemical vapor deposition (CVD), (3) carbonization of the hybrid sample to gain a carbon/silica nanocomposite, and (4) removal of the silica template. Diverse carbon sources have been involved in the synthesis, such as sucrose, furfuryl alcohol, phenol formaldehyde resin, benzene, poly-vinyl chloride, pitches, acenaphthene, propylene, acetonitrile, etc [3, 5, 9–13].

Many factors influence the final products, including the quality of hard templates, the filling amount, the carbonization process and more important, the carbon source. The first three issues have major effects on the mesostructures which have been intensively studied on the basis of a single carbon source. For example, the procedures have been given for the synthesis of highly ordered mesoporous carbons when sucrose [14], furfuryl alcohol [15, 16] or acenaphthene [12] is employed as a carbon source and mesoporous silica SBA-15 as a hard template. However, variable carbon sources may undergo different carbonization and therefore, derive discrepancy in both the mesostructure and graphitization. For instance, with the same SBA-15 template, unique tube-like OMCs can be easily obtained from furfuryl alcohol, but only rod-like products are gained from sucrose and acenaphthene. OMCs derived from acenaphthene show quite high graphitization. By comparison, those originated from sucrose and furfuryl alcohol display amorphous pore wall.

In this paper, we systematically investigated that the effects of carbon sources on the characters of OMCs such as mesostructures, surface areas, pore sizes and graphitization, and in turn on their electrochemical properties in electric double-layer capacitors (EDLCs). To minimize the effect of hard template, highly ordered SBA-15 from one batch is used. Four carbon sources, including sucrose, furfuryl alcohol, naphthalene and anthracene are involved in the syntheses on the basis of the reported procedures, which are proved to be efficient for nanocasting OMCs. Therefore, the discrepancies of final products are mainly caused by the carbon sources themselves. These carbon materials were characterized by X-ray powder diffraction (XRD), transmission electron microscopy (TEM) and N_2 adsorption. Their performances used as electrodes in EDLCs were measured with galvanostatic charge-discharge cycling and cyclic voltammetry (CV) curves.

2 Experimental section

2.1 Chemicals

Poly (propylene oxide)-*block*-poly (ethylene oxide)-*block*-poly (propylene oxide) triblock copolymer P123 (Mw = 5800, $EO_{20}PO_{70}EO_{20}$) was purchased from Acros Corp. Anthracene was purchased from Alfa Aesar Corp. Other chemicals were purchased from Shanghai Chemical Corp. All chemicals were used as received without any further purification. Millipore water was used in all experiments.

2.2 Samples

Mesoporous silica SBA-15 was synthesized as the reported procedure [17] except enlarging the amount by 10 times: 10.0 g of amphiphilic copolymer P123 was dispersed in 75 g of water and 300 g of 2 M HCl. 20.8 g of tetraethyl orthosilicate (TEOS, 98 wt%) was added to the homogeneous solution with stirring. The reaction was carried out at 38 °C for 24 h. The white milky solution was then transferred into autoclaves and aged at 100 °C for 3 days. After filtering without washing and drying at room temperature, the final products mesoporous silica SBA-15 were calcined at 550 °C for 5 h in air to decompose the triblock copolymer.

Sucrose, furfuryl alcohol, naphthalene and anthracene and the above prepared SBA-15 were used as the carbon sources and hard template, respectively, to prepare the OMCs by the nanocasting methods according to the previous papers [3, 18, 19]. The typical procedures are described as follows:

Sucrose-based mesoporous carbon was prepared by adding 0.5 g of SBA-15 to a solution obtained by dissolving 0.625 g of sucrose and 0.07 g of H_2SO_4 in 2.5 g of H_2O. The mixture was placed in an oven at 80 °C for 6 h, and subsequently heated at 160 °C for another 6 h. The resulted powders were put into the sucrose solution (0.375 g of sucrose, 0.04 g of H_2SO_4 and 2.5 g of H_2O) again for another impregnation cycle. After retreated at 80 and 160 °C again as before, complete carbonization was carried out in a furnace at 700, 900 and 1100 °C for 3 h, respectively, and 1300 °C for 2 h. The resultant mesoporous carbons were obtained by stirring carbon/silica composition in HF acid (10 wt%) for 24 h to remove the silica frameworks, filtering, washing and drying at room temperature.

About 0.5 g of furfuryl alcohol (90 wt%) and 0.05 g of oxalic acid were dissolved in 2.0 g of ethanol. The solution was then infiltrated into 0.5 g of SBA-15 by incipient wetness impregnation at room temperature, followed by polymerization at 80 °C overnight in the air and partial carbonization at 350 °C under N_2 for 6 h. The polymerization and carbonization processes were repeated again at 80 and 350 °C with another addition of 0.4 g of FA, 0.04 g of oxalic acid and 2.0 g of ethanol. The full carbonization and template removal were carried out as described above.

Typically, 0.2 g of naphthalene or 0.1 g of anthracene in 10 g of acetone containing 0.07 g of sulfuric acid was infiltrated into 0.5 g of SBA-15 templates at room temperature under stirring then partially pyrolyzed at 160 °C in the air. The impregnation and partial pyrolysis procedures were repeated until 1.0 g of naphthalene or 0.75 g of anthracene being consumed. The resultant composites were heated under N_2 atmosphere at 400 °C for 4 h, and then further carbonized as mentioned above.

The final carbon products are denoted as $C_{x\text{-}y}$, where x represents the carbon sources and y is the carbonization temperature. Here, suc, FA, npt and atr are used to simplify the precursors of sucrose, furfuryl alcohol, naphthalene and anthracene, respectively.

2.3 Characterization

Powder X-ray diffraction (XRD) patterns were recorded on a Bruker D4 powder X-ray diffractometer using Cu Kα radiation (40 kV, 40 mA). The unit cell parameters were calculated using the formula $a_0 = 2d_{100}/\sqrt{3}$, where d_{100} represents the d-spacing value of the 100 diffraction peak in XRD patterns. Transmission electron microscopy (TEM) images were taken on a JEOL JEM2011 electron microscope operating at 200 kV. For TEM measurements, the samples were prepared by dispersing the powder products as slurry in ethanol. Then they were dispersed and dried on a holey carbon film on a Cu grid for measurements. N_2 adsorption-desorption isotherms were measured with a Micromeritics Tristar 3000 analyzer at 77 K. Before the measurements, the samples were degassed at 180 °C for more than 5 h. The Brunauer–Emmett–Teller (BET) method was utilized to calculate the specific surface areas. The pore size distributions were derived from the adsorption branches of the isotherms based on the Barrett–Joyner–Halanda (BJH) model. The total pore volume, V_P, was estimated from the amount adsorbed at a relative pressure (P/P_0) of 0.99.

2.4 Electrochemical tests

Electrochemical measurements were preformed with a CHI 660A electrochemical workstation, using a three-electrode system. The mesoporous carbon products were used as the working electrodes with a platinum wire as the counter electrode, and a saturated calomel electrode (SCE) as the reference in a thermostat. The working electrode was a mixture of 95 wt% mesoporous carbon product (1.0 mg) and 5.0 wt% polytetrafluoroethylene (PTFE) binder. Cyclic voltammetry (CV) was conducted in 1.0 M H_2SO_4 solution at 25 °C with a scan rate of 50 mV/s. And the galvanostatic charge- discharge cycling test was performed galvanostatically at a current density of 0.1 mA/cm^2.

3 Results and discussion

3.1 Siliceous SBA-15 template

The small-angle XRD pattern for mesoprous SBA-15 template (Fig. 1a) shows five well-resolved peaks that can be indexed as 100, 110, 200, 210 and 300 reflections associated with 2D hexagonal symmetry (space group of *p*6 *mm*). The d_{100}-spacing is calculated to be 9.20 nm. A typical type-IV adsorption curve with a clear type-H1 hysteresis loop is observed in N_2 adsorption-desorption isotherms for SBA-15 (Fig. 1b). The sharp inflection of the isotherm in P/P_0 range from 0.60 to 0.80 is characteristic of capillary condensation within uniform pores. This silica template possesses a BET surface area of 590 m^2/g, a total pore volume of 1.10 cm^3/g and a pore size of 9.0 nm with a very narrow pore size distribution (Fig. 1b, inset). These results indicate the successful synthesis of highly ordered mesoporous silica SBA-15 hard template.

3.2 Ordered mesoporous carbons

3.2.1 Mesostructures

XRD patterns (Fig. 2a) for OMCs synthesized at 700 °C from different carbon precursors are similar and well-resolved, which suggest highly ordered 2D hexagonal mesostructure with the space group of *p*6 *mm*. Therefore, the mesostructures are retained fairly well after the nanocasting process regardless of carbon precursors. The d_{100}-spacing values of these OMCs (Table 1) are smaller than that of mesoporous silica SBA-15 template. This phenomenon is due to the framework shrinkage along with the emission of small molecules during the pyrolysis of carbon precursors.

When the carbonization temperature increases to 1300 °C, the dissimilarity is distinct for the OMCs synthesized from different carbon sources (Fig. 2b). In the cases of carbon sources of furfuryl alcohol and anthracene, three well-resolved peaks indexed as 100, 110 and 200 diffractions can be observed, assigned to 2D hexagonal *p*6 *mm* mesostructure. It indicates the maintenance of

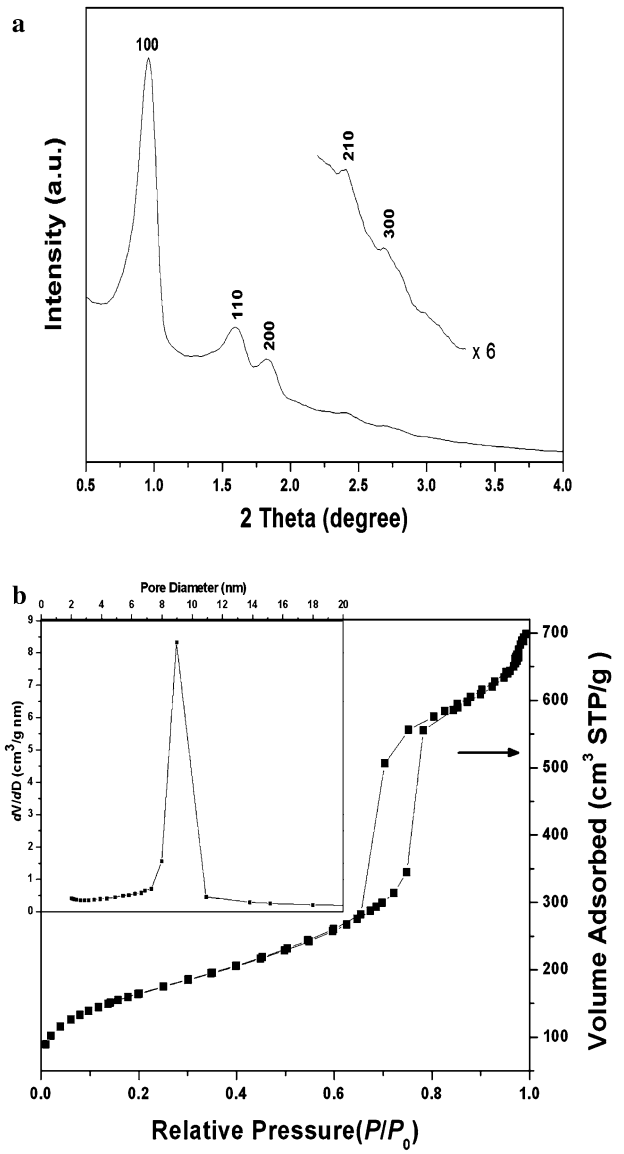

Fig. 1 Small-angle XRD pattern (**a**), nitrogen adsorption–desorption isotherms (**b**) and corresponding pore size distribution (**b**, inset) of mesoporous siliceous SBA-15 template

highly ordered mesostructure after high-temperature carbonization. The XRD pattern of $C_{suc\text{-}1300}$ gets less resolved, and the diffraction peaks ascribed to 110 and 200 diffractions weaken. This suggests a loss of mesoscopic ordering to some extent as sucrose is used as the precursor. For the OMC originated from naphthalene, the diffraction peaks broaden and the 110 and 200 reflections obviously weaken. The results indicate a severe decline in mesoscopic regularity.

Although the d_{100}-spacing values further reduce for all OMCs, this phenomenon is more serious for $C_{npt\text{-}1300}$. The d_{100}-spacing value decreases by 12.0%, almost twice larger than those of $C_{FA\text{-}1300}$ and $C_{atr\text{-}1300}$. $C_{suc\text{-}1300}$ displays a moderate reduction of 10.2%. This decreasing percentage reflects the framework shrinkage, which is caused by the gradual elimination of small molecules, in some cases, functional groups. It is obviously related to the carbon sources. From Table 1, it is also noticed that the framework shrinkage for OMCs prepared from sucrose and furfuryl alcohol reaches the plateau at the carbonization temperature of 1100 °C. Further increasing the temperature does not lead to any further shrinkage. For these two carbon sources, the functional groups such as carboxyls, anhydrides, lactones, hydroxyl, carbonyl, etc [20–22] deplete during the pyrolysis and carbonization at a temperature of 1100 °C. Few can survive at high temperatures.

TEM images of the OMCs (Fig. 3) show that $C_{FA\text{-}1300}$ and $C_{atr\text{-}1300}$ exhibit large domains of typically ordered strike-like and hexagonally arranged images. These results confirm highly ordered mesostructures and indicate the two OMCs well replicate the mesochannels of mesoporous silica SBA-15. TEM image of $C_{suc\text{-}1300}$ displays some stripe intermittent in pore walls, indicating the structure disfigurement. The evident deformation of hexagonal arrays in some domains for $C_{npt\text{-}1300}$ suggests the distinct decrease of mesostructure ordering, in accordance with the XRD result.

These behaviors clearly reveal that the carbon precursors of furfuryl alcohol and anthracene facilitate the formation of highly ordered mesoporous carbons from the nanocasting method with low framework shrinkage after high-temperature carbonization. When sucrose is employed as a carbon source, the regularity of resultant mesoporous carbon reduces to some extent, and the framework shrinkage is moderate. And naphthalene shows a low capability for truly replicating the mesochannels of SBA-15 at the high-temperature carbonization. Simultaneously, the framework shrinkage is relatively large. These differences may be originated from their nature. Furfuryl alcohol can easily polymerize to 3D continuous network in the acid catalyst; in addition, it is the main source of a typical thermosetting resin named furan resin that transforms to carbon with an extremely high yield upon carbonization [23, 24]. Therefore, it is common to demonstrate that the unique network of furfuryl alcohol can resist the loss of carbon atoms during the pyrolysis. Anthracene that has few hetero-atoms favors the high yield of carbon. The highly ordered mesostructures can be kept after high-temperature carbonization of these two compounds and the framework shrinkage is small. On the comparison, sucrose, which is rich of oxygen-containing groups could eliminate plentiful small molecules during the pyrolysis, and causes a relatively larger weight loss. The residual carbon after the carbonization is low due to the inevitable sublimation of naphthalene, in despite of the analogical molecular structure with anthracene. The carbon rods thin, therefore, it

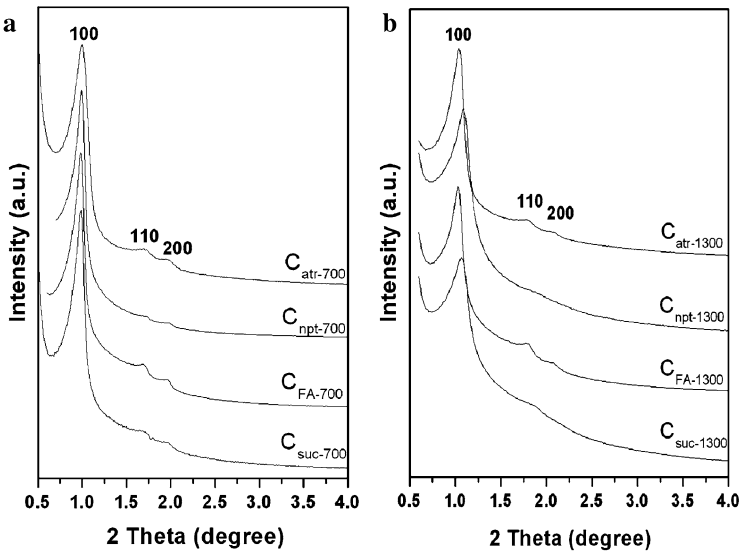

Fig. 2 Small-angle XRD patterns of the OMCs prepared by using siliceous SBA-15 as hard templates and sucrose, furfuryl alcohol, naphthalene and anthracene as carbon precursors after heating at 700 °C (**a**) and 1300 °C (**b**), respectively

Table 1 Textural properties of mesoporous carbon replicas using sucrose, furfuryl alcohol, naphthalene and anthracene as precursors and of their mother SBA-15 hard template

Sample	d_{100} (nm)	a_0 (nm)	D_{BJH} (nm)	V_P (cm^3/g)	S_{BET} (m^2/g)
SBA-15	9.20	10.6	9.0	1.10	590
$C_{suc-700}$	8.99	10.4	3.6	1.24	1300
C_{FA-700}	8.99	10.4	3.6	1.02	1070
$C_{npt-700}$	8.91	10.3	4.6	1.26	930
$C_{atr-700}$	8.82	10.2	3.8	0.49	530
$C_{suc-900}$	8.75	10.1	3.6	1.17	1440
C_{FA-900}	8.75	10.1	3.3	1.18	1230
$C_{npt-900}$	9.01	10.4	4.4	1.02	740
$C_{atr-900}$	8.92	10.3	4.3	0.70	560
$C_{suc-1100}$	8.26	9.5	3.8	1.02	1060
$C_{FA-1100}$	8.49	9.8	3.2	0.86	960
$C_{npt-1100}$	8.66	10.0	4.4	1.45	950
$C_{atr-1100}$	8.92	10.3	3.9	0.46	440
$C_{suc-1300}$	8.26	9.5	3.1	1.23	1470
$C_{FA-1300}$	8.58	9.9	3.1	1.04	1240
$C_{npt-1300}$	8.10	9.4	4.2	1.21	1130
$C_{atr-1300}$	8.49	9.8	4.0	0.38	450

d_{100} = d-spacing value of the 100 diffraction peak

a_0 = unit cell parameter

D_{BJH} = pore diameter

V_P = the total pore volume and S_{BET} = BET surface area

leads to the less ordered mesostructure and large framework shrinkage. Therefore, to get highly ordered mesoporous carbon, the carbon source is favorable that is of high resistance to severe conditions and of high yield to carbon.

Figure 4 depicts N_2 adsorption-desorption isotherms for the mesoporous carbon products carbonized at 1300 °C. All carbons represent type-IV curves (Fig. 4a). Well-defined and steep steps occur approximately at P/P_0 = 0.30–0.70 for $C_{FA-1300}$ and $C_{atr-1300}$. The behavior is associated with nitrogen filling of the mesopores owing to the capillary condensation, reflecting a high uniformity of mesopore sizes. This step is also distinct for $C_{suc-1300}$. The sample of $C_{npt-1300}$ does not exhibit a well-expressed adsorption step in nitrogen isotherms, suggesting a very wide distribution of mesopores. In addition, the continuous increase after the capillary condensation step indicates some textural (secondary) mesopores [25]. The pore-size distribution curves calculated from the adsorption branches confirm the results (Fig. 4b). $C_{FA-1300}$, $C_{atr-1300}$ and $C_{suc-1300}$ exhibit narrow pore-size distributions, which is characteristic of uniform mesopores. For $C_{npt-1300}$, the distribution curve is much wide. The heterogeneous mesopores reflect the deterioration of the mesostructure. The pore sizes are about 3–4 nm for all mesoporous carbons, larger than the wall thickness of mother SBA-15 material. It is common for the replicating materials due to the escape

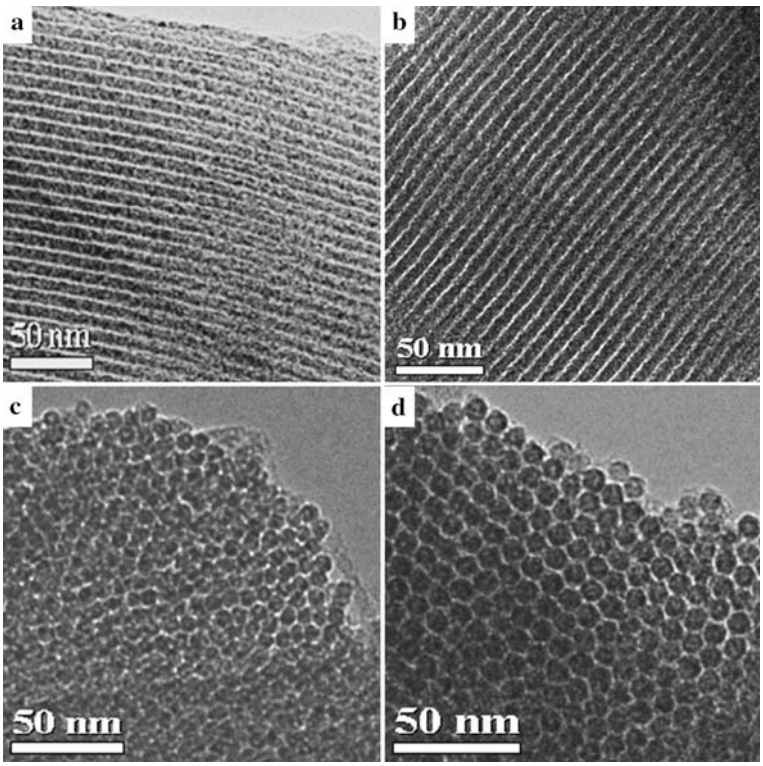

Fig. 3 TEM images of the OMCs carbonized at 1300 °C originated from sucrose (**a**), furfuryl alcohol (**b**), naphthalene (**c**) and anthracene (**d**), along the [001] (**a**, **b**) and [100] (**c**, **d**) directions

of solvents and the decomposition of precursors during carbonization, together with further lattice contraction after dissolution of silica [1, 3, 25–27]. The pore sizes of OMCs are not much related with the precursors, which can be attributed to the replication of the same SBA-15 walls. Although the structural shrinkage is different, it does not affect the mean pore sizes too much.

The BET surface areas and pore volumes for the carbons originated from different sources heated at different temperatures are listed in Table 1. It can be clearly seen that these two values are comparatively stable with a fluctuation to a little extent as a function of heating temperature for the carbons originated from one single source. This phenomenon is inconsistence with the variation of mesostructures. As the carbonization temperature increases, the structural shrinkage is more evident, and the mesoscopic regularity declines to some extent for some cases like $C_{suc\text{-}1300}$ and $C_{npt\text{-}1300}$. It indicates that these textual properties such as BET surface areas and pore volumes of mesoporous carbons are much related with the originated nature, instead of the mesostructural ordering.

Mesoporous carbons originated from sucrose, furfuryl alcohol and naphthalene have high surface areas and large pore volumes. For example, these two values are 1470 m^2/g and 1.23 cm^3/g respectively for $C_{suc\text{-}1300}$. $C_{atr\text{-}1300}$ exhibits a BET surface area and a pore volume as low as 450 m^2/g and 0.38 cm^3/g, respectively. This can be attributed to the fact that the anthracene with polyaromatic molecules affords OMC with extremely low microporosity after carbonization. On the other hand, the OMCs pepared from sucrose and furfuryl alcohol possess a large amount of irregular micropores located in the mesopore walls, after plentiful small molecules elimination from the carbon precursors during the carbonizaton. As reported previously, the micropores contributed significantly to the surface area and pore volume of OMCs [10, 25]. And it seems that both microporosity and secondary porosity, resulted from inevitable sublimation of naphthalene during pyrolysis, make the OMCs prepared from naphthalene have large surface area and pore volume. The high surface areas are important for the applications of OMCs in catalysis, adsorption, hydrogen storage, electrodes, etc [5, 28]. In order to obtain the OMCs with high surface areas, sucrose, furfuryl alcohol and naphthalene can be used as carbon sources.

3.2.2 Graphitic pore wall

Figure 5 shows wide-angle XRD patterns of the obtained OMCs. Three diffraction peaks at around 2θ = 22, 43 and 79° are observed in all XRD patters, corresponding to 002, 01 and 110 diffractions of carbon, respectively. Herein the 002 diffraction peak attributes to stacks of parallel layer planes [29]. The intensity of this diffraction peak is related to the numbers of the net planes in stacking. Its position denotes the inter-planar spacing and the reduced value reflects a growing ordering in the material. Therefore, the

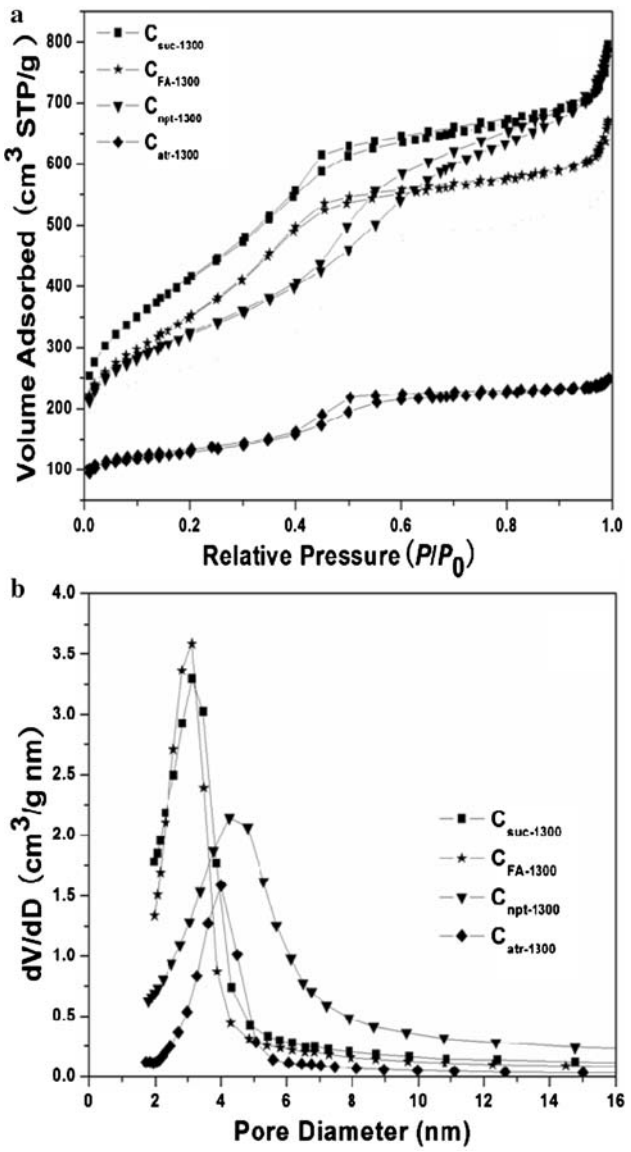

Fig. 4 Nitrogen adsorption–desorption isotherms of OMCs calcined at 1300 °C (**a**) and corresponding pore-size distribution curves (**b**)

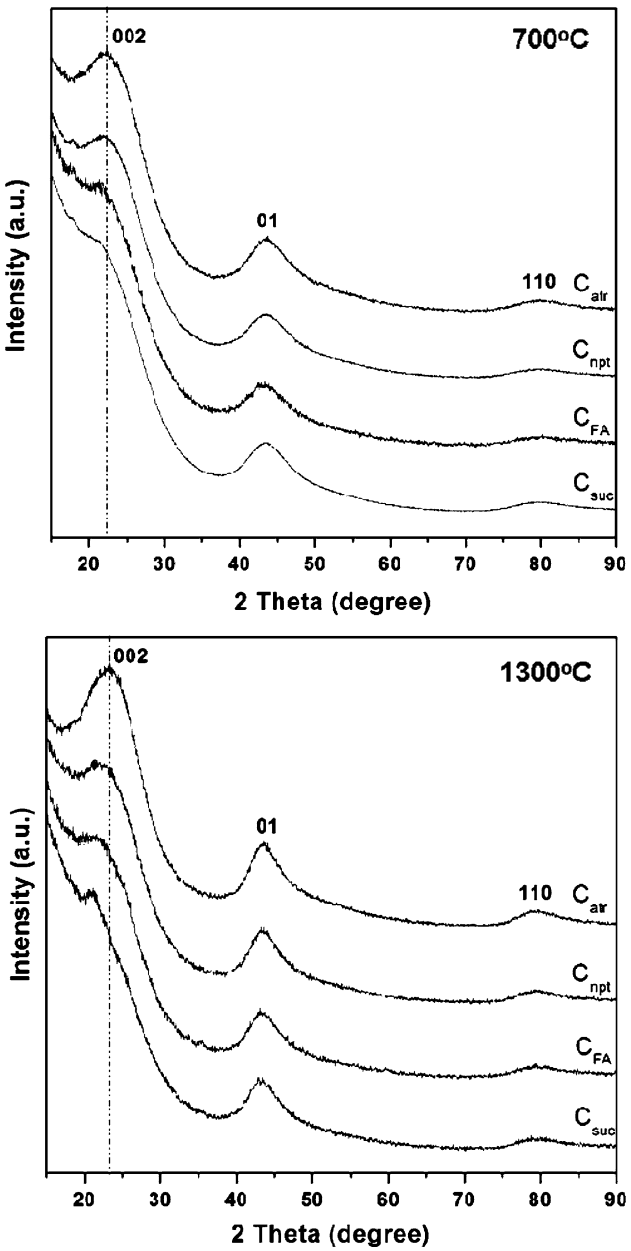

Fig. 5 Wide-angle XRD patterns of the mesoporous carbons originated from sucrose, furfuryl alcohol, naphthalene and anthracene calcined at 700 °C and 1300 °C, respectively

graphitic structure can be judged by the high intensity, narrow width and position of this peak. Among all OMCs carbonized at 700 °C, the mesoporous carbons originated from anthracene have the highest relative intensity and narrowest peaks for the 002 diffraction, indicating the highest graphitizing degree. This phenomenon is more evident with the increasing of carbonization temperature. The 002 diffraction for $C_{atr\text{-}1300}$ gets more resolved and narrower upon carbonization at 1300 °C, implying an enhancing graphitizing degree at high temperature. The d_{002} value of $C_{atr\text{-}1300}$ is 0.374 nm, a little larger than the value (0.342 nm) of graphitized carbon derived at 2800 °C [30]. It suggests that $C_{atr\text{-}1300}$ has a semi-graphitic structure. The material is not perfectly graphitized perhaps due to the low carbonization temperature. By comparison, $C_{npt\text{-}1300}$ can only be graphitized to a low degree. The OMCs prepared from sucrose and furfuryl alcohol maintain almost amorphous with extremely low graphitizing degrees even heated at 1300 °C, as evidenced by the wide 002 diffraction peak. In addition, for the latter three carbons, the carbonization temperature shows a minor effect on the 002 diffraction peak, and in turn, graphitizing degrees.

HRTEM images (Fig. 6) suggest that the walls of mesoporous carbon replicas are constructed with some

graphitic domains. This graphitized structure can be found along both the [001] and [100] directions owing to the irregular orientation of graphite layers. It is in accordance with the corresponding SAED patterns (Fig. 6, insets), which show a feature of polycrystalline materials. The OMC prepared with anthracene shows the highest graphitizing degree. As evidence, the graphitic structure can be easily found in a large region for $C_{atr\text{-}1300}$ (Fig. 6d), unlike the others whose graphite layers are mainly observed at the edges (Fig. 6a–c). The graphitizing degree is still not very high even in $C_{atr\text{-}1300}$, perhaps because of the low carbonization temperature. These results are in good agreement with the wide-angle XRD patterns.

The graphitization behaviors of organic compounds during carbonization have been systematically studied [31–36]. For carbon precursors (graphitizable and non-graphitizable), small graphite-like regions form the basic building blocks, containing a few graphitic layers joining together by cross-linkage. Several features are related with the subsequent graphitization. (1) The presence of sp^3-bonded atoms in non-graphitizing carbons resists to graphitization. (2) When the atomic basic structural blocks are randomly oriented and the cross-linkage is strong enough to prevent the movement of whole layers, the carbons are non-graphitizing. (3) In the case of nearly parallel blocks and weak cross-linkage between them, the structure can be easily transformed into graphite. (4) A high degree of the microtexture and large extent of the local molecular orientation are responsible for the ability to graphitize. The basic building blocks strongly cross-link for sucrose and furfuryl alcohol. The small graphite-like planes are roughly parallel and sometimes folded and twisted, which results in a disordered structure. This character, as well as the stable sp^3 bonds cause the OMCs prepared from these two carbons with extremely weak graphitic degrees. Anthracene has similar carbon atom arrangements of six-member aromatic rings to perfect graphite, and the strong π–π stacking interaction of the large conjugated system. The planar aromatic molecules are assembled to small stacking units with weak cross-linking, which would form quasi-aligned molecular units during pyrolysis. Although naphthalene has the analogous aromatic molecular framework, the derived carbon shows a low graphitic degree. It is possibly related to the special sublimation property of naphthalene. Graphitization is of great significance for electric conductivity. The carbon precursor of anthracene is suitable for fabricating graphitized OMCs.

3.2.3 *Electrochemical performance*

The capacitance study of materials for application as an electrochemical double-layered capacitor (EDLC) is considered as a promising high power energy source for portable electronic devices, cold-starting assistants and electric vehicles [37–39]. The applications of the obtained

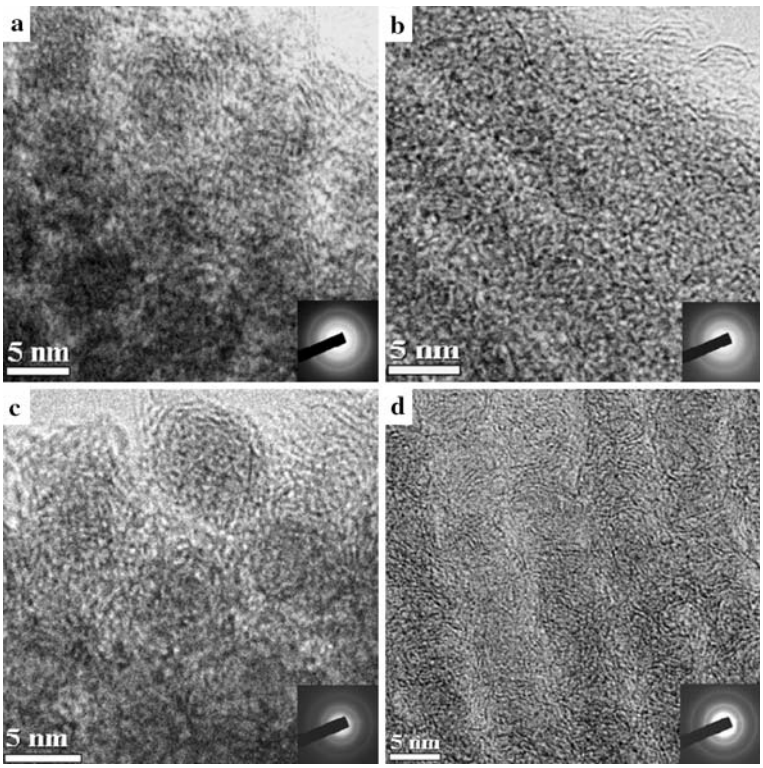

Fig. 6 HRTEM images of the OMCs carbonized at 1300 °C prepared from sucrose (**a**), furfuryl alcohol (**b**), naphthalene (**c**) and anthracene (**d**), along the [100] (**a**, **c**) and [001] (**b**, **d**) directions. Insets are corresponding SAED patterns of the observed domains

OMCs as electrodes in EDLCs are measured with galvanostatic charge–discharge cycling and cyclic voltammetry (CV) curves.

Figure 7 plots the specific capacitances on the basis of galvanostatic charge–discharge cycling for these OMCs as a function of the carbonization temperature. For the OMCs carbonized at 700 °C, $C_{suc\text{-}700}$ and $C_{FA\text{-}700}$ display high specific capacitances of about 189 and 178 F/g, respectively. The capacitance of $C_{npt\text{-}700}$ is 99 F/g, and $C_{atr\text{-}700}$ exhibits a low specific capacitance of 19 F/g. When the carbonization temperature increases, EDLC behaviors are different. The capacitances of OMCs originated from sucrose and furfuryl alcohol initially reduce in the carbonization temperature range of 700–1100 °C and then reach a constant. A continuous improvement of EDLC performance is detected for the OMCs prepared from anthracene in the experimental temperature range. In the case of the OMC from naphthalene, the specific capacitance almost keeps a constant.

As CV curves of OMCs carbonized at 700 and 1100 °C (Fig. 8) show, rectangle-shaped curves are clearly observed for all OMCs with a high scan rate of 50 mV/s. It indicates the comparatively ideal charge/discharge processes of EDLC properties. The integral areas under the CV curves express their specific capacitances. In the cases of OMCs heated at 700 °C, $C_{suc\text{-}700}$ and $C_{FA\text{-}700}$ reveal the highest capacitances. $C_{atr\text{-}700}$ displays the lowest capacitance and $C_{npt\text{-}700}$ has a medium one. The variation of capacitances of these OMCs along the carbonization temperature is presented as a visible reduction for $C_{suc\text{-}1100}$ and $C_{FA\text{-}1100}$, maintenance for the OMC originated from naphthalene and a steady enhancement for $C_{atr\text{-}1100}$. These phenomena are coincident with the galvanostatic charge-discharge cycling results.

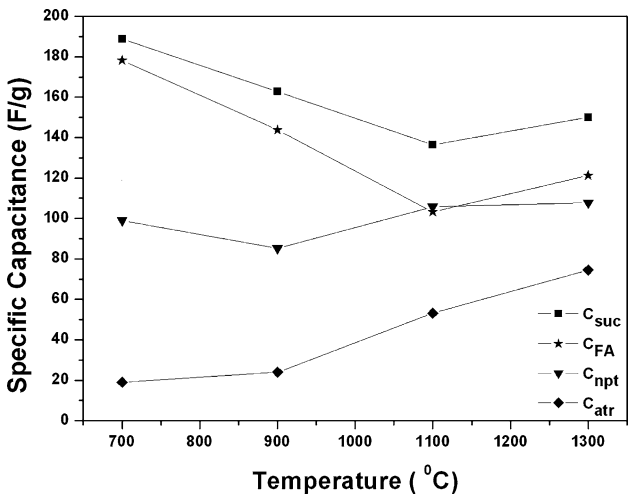

Fig. 7 Specific capacitances for the OMCs prepared by using surose, furfuryl alcohol, naphthalene and anthracene as precursors carbonized at 700, 900, 1100, and 1300 °C, respectively

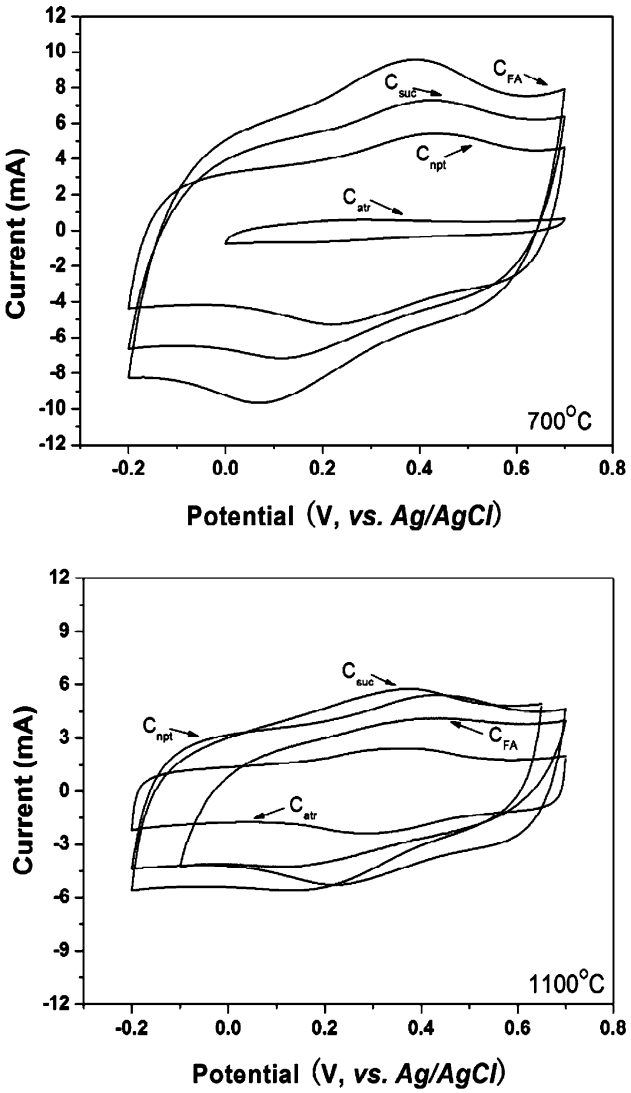

Fig. 8 Cyclic voltammetry curves of ordered mesoporous carbons calcined at 700 and 1100 °C, respectively

EDLCs utilize the electric double layer formed at the electrode/electrolyte interface for charge storage. The performance of which must be integrative reflects of many factors [40–43]. In general, as a good practical EDLC, the electrode material should simultaneously possess high surface areas for charge storage, large and uniform pore size to facilitate high-speed ion diffusion, suitable surface functional groups to enhance the wettability to the electrolyte and good electric conductivity to ensure the complete utilization of electrode surface especially in high current (rate) conditions. When the OMCs are prepared at low temperature, such as 700 °C, all carbon materials except $C_{atr\text{-}700}$ have very low graphitic degrees. Even for the latter, the graphitic degree is not high. In addition, the

pore sizes are close. Therefore, the functional groups and surface areas play the dominant roles in the EDLC performances. The OMCs originated from sucrose and furfuryl alcohol have abundant electroactive functional groups and high surface areas, which have good accessibility to electrolyte and charge storage. Indeed the pseudocapacitances appeared at 0.1–0.6 V (vs SCE) for $C_{suc\text{-}700}$ and $C_{FA\text{-}700}$ are related to charge-transfer redox reactions of the functional groups at the carbon surfaces [37, 42]. It is reasonable that $C_{atr\text{-}700}$ possesses a low capacitance due to both the low surface area and the lack of functional groups. The latter is estimated from the negligible pseudocapacitances. With a high surface area and the absence of functional groups, $C_{npt\text{-}700}$ has a medium capacitance. Accompanied with the increasing of carbonization temperature, the features of OMCs vary. The functional groups gradually eliminate, and the BET surface areas almost keep the same. The graphitic degree is improved for the OMC originated from anthracene while the degrees are preserved for the other three kinds of carbons. Consequently, EDLC performances are initially declined in the cases of the OMCs using sucrose and furfuryl alcohol as precursors due to the loss of functional groups, and then unchanged caused by the relatively stable properties at high temperatures. It is steadily increasing for C_{atr} possibly due to the enhancing graphitic degree and the retention of highly ordered mesostructure. As the OMCs prepared from naphthalene are concerned, the capacitance maintains a constant owing to almost unchangeable properties, including BET surface area and graphitic degree.

4 Conclusions

Ordered mesoporous carbons were prepared using well-reported nanocasting procedures from mesoporous silica SBA-15 hard template and sucrose, furfuryl alcohol, naphthalene and anthracene precursors. All obtained OMCs fully replicated 2D hexagonal pore channels of SBA-15, resulting highly ordered mesostructures with *p*6 *mm* space group. Their different properties reflect the effects of carbon sources on the final products. Highly ordered mesostructures can be well retained even at a high carbonization temperature of 1300 °C when the precursors with high resistance to severe conditions and high yields to carbons are involved, for example, furfuryl alcohol and anthracene. Mesoporous carbons originated from non-graphitizable carbon sources like sucrose and furfuryl alcohol, have amorphous pore walls and large surface areas and pore volumes. But the pore sizes of OMCs are close regardless of the precursors that can be attributed to the replication of the same SBA-15 pore walls and the minor effects of structural shrinkage on mean pore sizes. To get OMCs with graphitic walls, the precursors are suitable that have nearly parallel blocks with weak cross-linkage and local molecular orientation like anthracene. But the precursors with some special characters, such as sublimation should be occluded. When the OMCs are applied as electrodes in EDLCs, the properties including surface areas, pore sizes, graphitic pore walls and functional groups should be synthetically considered. OMCs synthesized using sucrose and furfuryl alcohol as precursors with high surface areas and abundant functional groups show large capacitances, which will be reduced with the elimination of eletroactive groups at high carbonization temperatures. The improving graphitic degrees with the increasing of carbonization temperature of the OMCs from anthracene offer them a gradual enhancement of capacitances, although the capacitance is very low at low temperature due to the low surface area and lack of functional groups. For naphthalene derived OMCs, the stable properties such as relatively high surface areas, few electroactive groups and limited graphitizable properties result in medium but almost constant capacitances. This work illuminates that, the nature of precursors affect the structural characteristics including mesoscopic regularity, surface areas, pore volumes, graphitic degrees, functional groups, and in turn, the practical applications.

Acknowledgment This work was supported by NSF of China (20407014, 20421303, 20373013 and 20521140450); State Key Basic Research Program of PRC (2006CB202502); Shanghai Sci. & Tech. Committee (06DJ14006, 055207078, 05DZ22313, and 03QF14037); Shanghai Nanotech Promotion Center (0652nm024), Shanghai Education Committee (02SG01, 04DB05 and T0402); Program for New Century Excellent Talents in University (NCET-04-03). We thank Dr. S. H. Xie for TEM assistance. Y. W. thanks the China Post-Doc Scientific Fund.

References

1. R. Ryoo, S.H. Joo, S. Jun, J. Phys. Chem. B. **103**, 7743 (1999)
2. R. Ryoo, S.H. Joo, M. Kruk, M. Jaroniec, Adv. Mater. **13**, 677 (2001)
3. S. Jun, S.H. Joo, R. Ryoo, M. Kruk, M. Jaroniec, Z. Liu, T. Ohsuna, O. Terasaki, J. Am. Chem. Soc. **122**, 10712 (2000)
4. M. Kaneda, T. Tsubakiyama, A. Carlsson, Y. Sakamoto, T. Ohsuna, O. Terasaki, S.H. Joo, R. Ryoo, J. Phys. Chem. B. **106**, 1256 (2002)
5. S.H. Joo, S.J. Choi, I. Oh, J. Kwak, Z. Liu, O. Terasaki, R. Ryoo, Nature **412**, 169 (2001)
6. J. Lee, S. Yoon, T. Hyeon, S.M. Oh, K.B. Kim, Chem. Commun. **2177**, (1999)
7. J.S. Lee, S.H. Joo, R. Ryoo, J. Am. Chem. Soc. **124**, 1156 (2002)
8. H.F. Yang, Q.H. Shi, X.Y. Liu, S.H. Xie, D.C. Jiang, F.Q. Zhang, C.Z. Yu, B. Tu, D.Y. Zhao, Chem. Comm. **2842**, (2002)
9. J. Lee, K. Sohn, T. Hyeon, J. Am. Chem. Soc. **123**, 5146 (2001)
10. H.F. Yang, Y. Yan, Y. Liu, F.Q. Zhang, R.Y. Zhang, Y. Meng, M. Li, S.H. Xie, B. Tu, D.Y. Zhao, J. Phys. Chem. B. **108**, 17320 (2004)

11. A.B. Fuertes, S. Alvarez, Carbon. **42**, 3049 (2004)
12. T.W. Kim, I.S. Park, R. Ryoo, Angew. Chem. Int. Ed. **42**, 4375 (2003)
13. Y.D. Xia, Z.X. Yang, R. Mokaya, J. Phys. Chem. B. **108**, 19293 (2004)
14. K. Bohme, W.D. Einicke, O. Klepel, Carbon. **43**, 1918 (2005)
15. M. Kruk, M. Jaroniec, T.W. Kim, R. Ryoo, Chem. Mater. **15**, 2815 (2003)
16. A.H. Lu, W. Schmidt, B. Spliethoff, F. Schuth, Adv. Mater. **15**, 1602 (2003)
17. D.Y. Zhao, J.L. Feng, Q.S. Huo, N. Melosh, G.H. Fredrickson, B.F. Chmelka, G.D. Stucky, Science. **279**, 548 (1998)
18. A.H. Lu, W.C. Li, W. Schmidt, W. Kiefer, F. Schuth, Carbon. **42**, 2939 (2004)
19. C.H. Kim, D.K. Lee, T.J. Pinnavaia, Langmuir **20**, 5157 (2004)
20. Y.S. Lim, H.S. Kim, M.S. Kim, N.H. Cho, S. Nahm, Macromole. Res. **11**, 122 (2003)
21. D.J. Kim, H.I. Lee, J.E. Yie, S.J. Kim, J.M. Kim, Carbon. **43**, 1868 (2005)
22. E.B. Sanders, A.I. Goldsmith, J.I. Seeman, J. Anal. & Appl. Pyroly. **66**, 29 (2003)
23. S.M. Manocha, D.Y. Vashistha, L.M. Manocha, J. Mater. Sci. Lett. **16**, 705 (1997)
24. A. Shindo, K. Izumino, Carbon **32**, 1233 (1994)
25. K.P. Gierszal, T.W. Kim, R. Ryoo, M. Jaroniec, J. Phys. Chem. B. **109**, 23263 (2005)
26. T.W. Kim, Ryoo, R.K. P. Gierszal, M. Jaroniec, L.A. Solovyov, Y. Sakamoto, O. Terasaki, J. Mater. Chem. **15**, 1560 (2005)
27. Y. Sakamoto, T.W. Kim, R. Ryoo, O. Terasaki, Angew. Chem. Int. Ed. **43**, 5231 (2004)
28. F. Schuth, Angew. Chem. Int. Ed. **42**, 3604 (2003)
29. V.A. Davydov, A.V. Rakhmanina, V. Agafonov, B. Narymbetov, J.P. Boudou, H. Szwarc, Carbon. **42**, 261 (2004)
30. I. Mochida, Y. Korai, C.H. Ku, F. Watanabe, Y. Sakai, Carbon. **38**, 305 (2000)
31. A. Burian, P. Daniel, S. Duber, J. Dore, Philosophical Magazine B. **81**, 525 (2001)
32. P.J.F. Harris, Int. Mater. Rev. **42**, 206 (1997)
33. S. Ergun, V.H. Tiensuu, Acta Crystallogr. **12**, 1050 (1959)
34. S. Ergun, L.E. Alexander, Nature **195**, 765 (1962)
35. A. Oberlin, Carbon **22**, 521 (1984)
36. J.N. Rouzaud, A. Oberlin, Carbon **27**, 517 (1989)
37. E. Frackowiak, F. Beguin, Carbon **39**, 937 (2001)
38. M. Winter, R.J. Brodd, Chem. Rev. **104**, 4245 (2004)
39. A.S. Arico, P. Bruce, B. Scrosati, J.M. Tarascon, W. Van Schalkwijk, Nature Mater. **4**, 366 (2005)
40. H.Y. Liu, K.P. Wang, H.S. Teng, Carbon **43**, 559 (2005)
41. A.B. Fuertes, F. Pico, J.M. Rojo, J. Power Sources **133**, 329 (2004)
42. S. Yoon, J.W. Lee, T. Hyeon, S.M. Oh, J. Electrochem. Soc. **147**, 2507 (2000)
43. K.L. Yang, S. Yiacoumi, C. Tsouris, J. Electroanal. Chem. **540**, 159 (2003)